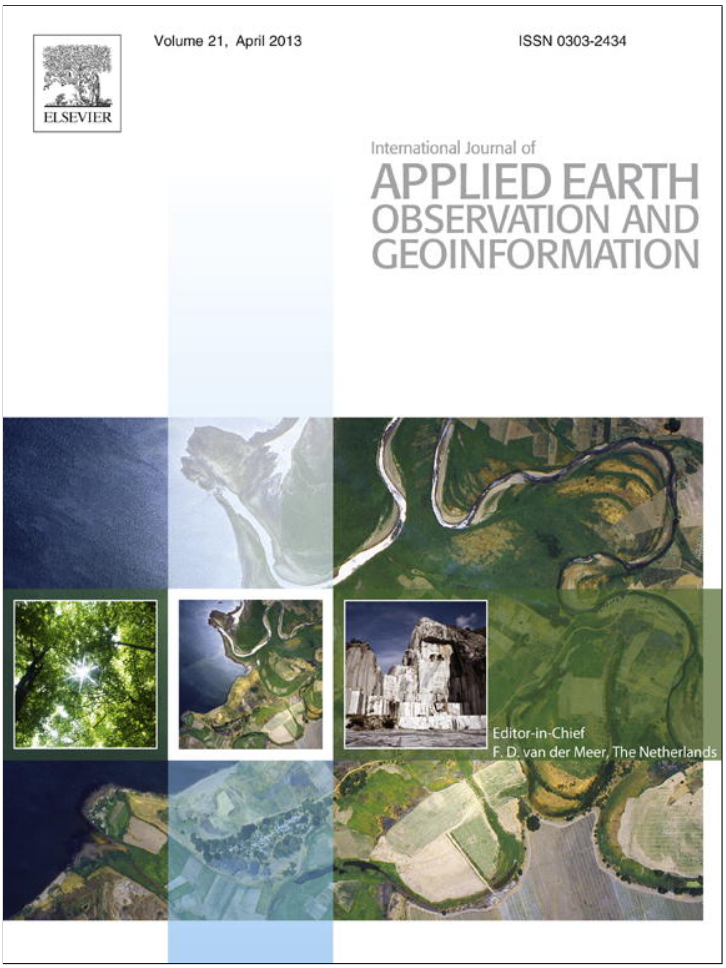

International Journal of Applied Earth Observation and Geoinformation 21 (2013) 427–435

Contents lists available at SciVerse ScienceDirect

International Journal of Applied Earth Observation and Geoinformation

journal homepage: www.elsevier.com/locate/jag

Assessing geometric accuracy of the orthorectification process from GeoEye-1 and WorldView-2 panchromatic images

Manuel A. Aguilar*, María del Mar Saldaña, Fernando J. Aguilar

Department of Agricultural Engineering, Almería University, Ctra. de Sacramento s/n, La Cañada de San Urbano, Escuela Superior de Ingeniería, 04120 Almería, Spain

ARTICLE INFO

Article history:
Received 17 February 2012
Accepted 8 June 2012

Keywords:
Very high resolution satellite images
Sensor model
Rational functions
Geopositioning accuracy
Orthorectification

ABSTRACT

GeoEye-1 and WorldView-2 are the commercial very high resolution (VHR) satellites more innovative, unexplored and presenting the highest available resolutions nowadays. The attainable geopositioning accuracies from GeoEye-1 and WorldView-2 single panchromatic images, both along the sensor orientation and orthorectification phases, are analyzed at the same study area and by using exactly the same ancillary data. The accuracy assessment was carried out depending on the following factors: (i) type of input satellite image (GeoEye-1 Geo, WorldView-2 Ortho Ready Standard and WorldView-2 Basic), (ii) sensor orientation model used (rigorous and based on rational function), (iii) number of well-distributed ground control points (GCPs) used in the triangulation process, (iv) off-nadir viewing angle, and finally (v) vertical accuracy of the DEM employed to conduct the orthorectification process.

Regardless of satellite or product, the best horizontal geopositioning accuracies were always attained by using third order 3D rational functions with vendor's rational polynomial coefficients data refined by a zero order polynomial adjustment (RPC0). Focusing on WorldView-2 products, worse accuracies were yielded from Basic images than from Ortho Ready Standard level ones.

As a general rule, and for attaining sub-pixel planimetric accuracies for the orthorectified GeoEye-1 Geo and WorldView-2 Ortho Ready Standard images and using RPC0 model with 7 GCPs, users should avoid off-nadir angles higher than 20° and use a very accurate DEM.

1. Introduction

Orthorectification of satellite data is one of the most important pre-processing steps for mapping applications, for identifying a broader range of land or urban features (i.e., image classification) and for adding georeferenced image data into Geographic Information Systems. In this way, the recent advent of the first very high resolution (VHR) satellites, capable of capturing panchromatic (PAN) imagery of the land surface with Ground Sample Distance (GSD) even lower than 1 m, marks a new era in the field of remote sensing. Although many VHR satellites have been successfully launched during the last decade, nowadays the couple of commercial VHR satellites more innovative and unexplored are GeoEye-1 (GeoEye, Inc.) and WorldView-2 (DigitalGlobe, Inc.), launched in September 2008 and October 2009 respectively. Many studies have been carried out in applications of these new breed of VHR remote sensing images (e.g., Dennison et al., 2010; Ozdemira and Karnieli, 2011). Currently, GeoEye-1 is the commercial satellite with the highest geometric resolution, with 0.41 m GSD at nadir in PAN imagery and 1.65 m GSD at nadir in multispectral (MS) imagery. On the other hand, WorldView-2 has the ability to collect PAN and MS images (the first VHR commercially available 8-band MS satellite) with pixel size of 0.46 m and 1.84 m at nadir respectively. However, image products from GeoEye-1 and WorldView-2 have to be down-sampled to 0.5 m and 2 m in PAN and MS respectively for commercial sales, as a requirement levied by the U.S. Government.

Users can produce their own highly accurate orthorectified images by utilizing commercial off-the-shelf software and ancillary data such as digital elevation models (DEMs) and ground control points (GCPs) through VHR satellite imagery available as (i) Basic images (very close to the original images) or (ii) images projected to a plane with constant height (map-projected level). DigitalGlobe's VHR satellites are available in both, Basic product and Ortho Ready Standard Level-2A (ORS2A) images (DigitalGlobe, 2010), whereas GeoEye's ones (GeoEye, 2009) only are attainable as map-projected level (Geo images). The first step for carried out the orthorectified process would be the triangulation or sensor orientation whereas the final product would be generated by removing the distorting affects of the terrain relief using a proper DEM. In the last decades, several mathematical models for VHR satellite sensor orientation and 3D geopositioning supported on 3D GCPs have been tested. These models can be categorized into two main groups:

* Corresponding author. Tel.: +34 950015997; fax: +34 950015491.
E-mail addresses: maguilar@ual.es (M.A. Aguilar), msd452@ual.es (M.M. Saldaña), faguilar@ual.es (F.J. Aguilar).

0303-2434/$ – see front matter © 2012 Elsevier B.V. All rights reserved.
http://dx.doi.org/10.1016/j.jag.2012.06.004

(i) 3D rigorous or physical mathematical models which can present accurately the satellite sensor motion in space and the relationship between the satellite image space and the ground space. The use of this group of models depends on the availability and quality of the sensor information and the satellite ephemeris data. Therefore, the form of the rigorous mathematical models may be changed from one sensor to another. DigitalGlobe's Basic images are delivered with a set of metadata files including full information about attitude and ephemeris data, geometric calibration and camera model. Because of these, many physical sensor models only work on this type of images (e.g., Dolloff and Settergren, 2010; Deltsidis and Ioannidis, 2011). In previous studies, rigorous sensor models have proved to be the best option for QuickBird Basic images (e.g., Wolniewicz, 2004; Aguilar et al., 2007). However, they did not work so well on Ikonos or GeoEye-1 Geo images (Wolniewicz, 2004; Aguilar et al., 2008a; Crespi et al., 2010; Aguilar et al., 2012). More recently, Capaldo et al. (2012) compared two different rigorous sensor models with stereo pairs of WorldView-1 (the WorldView-2's older sister satellite) and GeoEye-1. In both cases and after the sensor orientation phase, SISAR software, developed at the Area di Geodesia e Geomatica (Università di Roma, La Sapienza), achieved better results than a 3D physical model included within PCI Geomatica OrthoEngine (PCI Geomatics, Richmond Hill, Ontario, Canada). However, these results were supported in an extremely small number of Independent Check Points (ICPs).

(ii) Empirical models that can approximate the relationship between the image and the object spaces without any information about the sensor motion in space, the satellite ephemeris or attitude data. In the absence of that complete information, rational functions are introduced by many investigators as mathematical model for image to ground coordinate system transformation in a conventional way (e.g., Tao and Hu, 2001; Grodecki and Dial, 2003; Fraser and Hanley, 2005) or in an innovative way (e.g., Valadan Zoej et al., 2007). The well-known vendor supplied rational polynomial coefficients (RPCs), compensated in image space using a modest number of high accurate 3D GCPs, is the most widely used sensor model for VHR satellite imagery. In this way, using bias-corrected RPCs model and a single GCP, extremely accurate geopositioning results, clearly much better than those attained by using older satellites such as Ikonos or QuickBird, were reported by Fraser and Ravanbakhsh (2009) working on a stereo pair of GeoEye-1.

The main objective of this paper was to compare, exactly in the same conditions, the geopositioning accuracy capabilities of GeoEye-1 (Geo product) and WorldView-2 (ORS2A and Basic products) PAN singles images for generating orthorectified imagery under an operational environment. In this sense, a statistical analysis was performed for studying the following variation sources: (i) type of input VHR PAN satellite image, (ii) sensor orientation model used, (iii) number of well-distributed GCPs used in the triangulation process, (iv) off-nadir viewing angle, and finally (v) accuracy of the DEM employed in the orthorectification process.

2. Study site and data set

2.1. Study site

The study area is centered on WGS84 geographic coordinates of 37.2109° North and 1.8027° West and it comprises a coastal fringe of Almería (Southern Spain), approximately 11 km long and 775 m wide (Fig. 1). The study area presents a smooth relief, with heights ranging from 0 m to 55 m and a mean value close to 7 m.

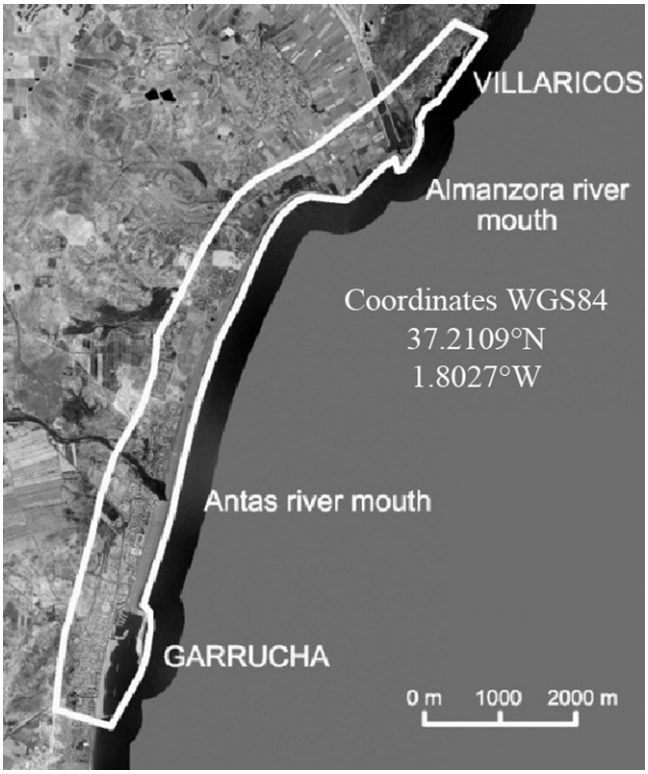

Fig. 1. Location of the study site on the Almería coast, Spain.

2.2. Remote sensing data

During 2010 and 2011, eight VHR satellite PAN images covering the study area (three GeoEye-1 Geo images, three WorldView-2 ORS2A and two WorldView-2 Basic images) were acquired. All these images were finally down-sampled to 0.5 m GSD. The characteristics of all of them are shown in Table 1.

2.2.1. GeoEye-1 data

For GeoEye-1, only images projected to a surface with constant height are distributed as Geo images. In fact, GeoEye-1 Geo is the GeoEye's commercial imagery format that presents the least level of corrections, both radiometric and geometric. Geo images are shipped with the sensor camera model in RPCs format and a metadata file. In the last file the most relevant physical parameters of the image are summarized. The Geo product permits skilled users to make orthorectified products using standard commercial software (GeoEye, 2009).

For this work three GeoEye-1 Geo images were acquired. The first one was taken on September 29, 2010, occupying approximately 49 km^2. On August 27, 2011, a GeoEye-1 GeoStereo product was taken, containing two images which counted on the appropriate stereo geometry to support a wide range of stereo imagery applications such as DEMs creation. In a single image, GeoStereo product is identical to Geo product. Therefore, due to the fact that only single images were going to be computed along this work, we will refer to the GeoStereo and Geo images without any difference from now on. An area of 100 km^2 was ordered for both images taken in August 2011, always including the aforementioned working area.

2.2.2. WorldView-2 data

Through the DigitalGlobe's WorldView-2 (WV-2) satellite images, users can produce their own highly accurate orthorectified products by utilizing commercial off-the-shelf software and ancillary data such as DEMs and GCPs. For this task, the two

Table 1
Characteristics of panchromatic images from GeoEye-1 (Geo and GeoStereo products) and WorldView-2 (ORS2A and Basic products) acquired at the study site.

Product	GeoEye-1 Geo	GeoEye-1 GeoStereo	GeoEye-1 GeoStereo	WV-2 ORS2A	WV-2 ORS2A and Basic	WV-2 ORS2A and Basic
Acquisition date	29/09/2010	27/08/2011	27/08/2011	19/07/2011	18/08/2011	18/08/2011
Acquisition time (GTM)	11:01	10:55	10:56	11:23	11:22	11:23
Cloud cover	0%	0%	0%	0%	0%	0%
Scan direction	Reverse	Reverse	Reverse	Forward	Forward	Reverse
Sun azimuth	159.3°	144.1°	144.4°	142.5°	152.3°	152.8°
Sun elevation	48.4°	58.3°	58.4°	70.5°	63.7°	63.8°
Collection elevation	69.4°	81.5°	66.9°	85.0°	67.6°	80.0°
Collection azimuth	221.9°	40.4°	183.6°	279.9°	4.7°	216.1°
Collected Col GSD	0.460 m	0.416 m	0.480 m	0.467 m	0.499 m	0.473 m
Collected Row GSD	0.449 m	0.417 m	0.440 m	0.465 m	0.538 m	0.480 m
Product pixel size	0.5 m	0.5 m	0.5 m	0.5 m	0.5 m	0.5 m

more appropriated WV-2 products would be both ORS2A and Basic imagery (DigitalGlobe, 2010).

DigitalGlobe's Basic imagery products are the most radiometrically and sensor corrected, but not geometrically corrected or mapped to a cartographic projection and ellipsoid. These Basic products are close to the raw images presents the least level of corrections from DigitalGlobe's satellite imagery. Basic imagery comes accompanied by Image Support Data (ISD) files which include full information about attitude and ephemeris data, geometric calibration, camera model and rational polynomial coefficients.

WV-2 ORS2A images present both radiometric and geometric corrections in a similar level to the GeoEye's Geo format. ORS2A images are georeferenced to a cartographic projection using a surface with constant height and, as in the case of GeoEye's Geo level, they include the corresponding RPC sensor camera model and a very limited metadata file.

On August 18, 2011, a WV-2 Basic Stereo pair was acquired containing two PAN Basic scenes, both covering the same 210 km^2 and including the working area. Both aforementioned Basic images were also ordered in ORS2A format but only over 49 km^2. Besides these four images, a WV-2 ORS2A PAN image was acquired on July 19, 2011, also covering the whole working area with 49 km^2.

2.3. Ground points collection

The coordinates of 44 GCPs and 75 ICPs were obtained by differential global positioning system (DGPS) using a total GPS Topcon HiPer PRO station working in real time kinematic mode (RTK). GCPs were used only to compute the different sensor models which will be presented later, whereas ICPs were only applied in the accuracy assessment. Both GCPs and ICPs, located on well-defined features and homogeneously distributed over the study area (Fig. 2), were measured with reference to the European Terrestrial Reference System 1989 (ETRS89) and UTM projection. The vertical datum took the geoid as the reference surface, adopting the mean sea level in the calm seas of Alicante (Spain) as the null orthometric height point. The goal was to obtain a reliable measurement of GCPs and ICPs with accuracy better than a decimeter.

A previous geopositioning accuracy assessment of GeoEye-1 PAN and MS image was carried out by Aguilar et al. (2012) using the aforementioned single bundle GeoEye-1 Geo image taken in September 2010. Because of that, more detailed information about the materials and methods used here can be found in that paper.

2.4. Digital elevation models

Two DEMs were tested along the orthorectification process for the generation of orthoimages from the GeoEye-1 and WV-2 images:

(i) A high accuracy and 1 m grid spacing LiDAR-derived DEM. This DEM was taken in 2009 using a Leica ALS60 airborne laser scanner with 35° field of view (FOV) and the support of a nearby ground GPS reference station. The estimated vertical RMSE computed from 62 ICPs, took a value close to 8.9 cm.
(ii) As high accurate LiDAR-derived DEMs are not always available, a medium resolution 10 m grid spacing DEM covering the whole area of Andalusia, generated and published by the Andalusia Government (Andalusia Government, 2005) from a B&W photogrammetric flight at an approximate scale of 1:20,000. This DEM presented a vertical accuracy measured as root mean square error (RMSE) of 1.34 m, computed upon 62 DGPS high accuracy ICPs located at open terrain and distributed over the whole working area.

Fig. 2. Distribution of 75 ICPs (black crosses) and 44 GCPs (white circles) overlaid on a GeoEye-1 panchromatic orthorectified image.

3. Methodology

3.1. Sensor models tested

In satellite imagery, geometric sensor models are used to relate the relationship between the three-dimensional (3D) object space positions (X, Y, Z) to their corresponding two dimensional (2D) image space positions (x, y). Two different kinds of sensor models supported on 3D GCPs have been tested:

(i) A 3D physical model developed by Toutin (2003) at the Canada Centre for Remote Sensing (CCRS) and embedded within the commercial software PCI Geomatica OrthoEngine v 10.3.2.
(ii) Three sensors model based on the well-known rational functions using vendor supplied RPCs and compensated in image space using a few number of high accurate 3D GCPs were tested too. The RPC's models are based on ratios of polynomials (Eq. (1)), where x and y are the row and column in the image space respectively, X, Y, and Z are the coordinates of points in object space, and, P_i (i = 1–4) are third order polynomial functions (Eq. (2)), being c_{ii} the vendor supplied RPCs (Tao and Hu, 2001).

$$x = \frac{P_1(X, Y, Z)}{P_2(X, Y, Z)} \qquad y = \frac{P_3(X, Y, Z)}{P_4(X, Y, Z)} \tag{1}$$

$$P_i = c_{1i} + c_{2i}X + c_{3i}Y + c_{4i}Z + c_{5i}XY + \cdots + c_{17i}YZ^2 + c_{18i}X^2Z + c_{19i}Y^2Z + c_{20i}Z^3 \tag{2}$$

A complementary transformation based on a few GCPs is essential for attained the best accuracies. The OrthoEngine's RPC indirect method is based on the block adjustment method developed by Grodecki and Dial (2003) for image space (Eq. (3)):

$$\Delta x = x' - x = a_0 + a_1 \cdot x + a_2 \cdot y + a_3 \cdot x \cdot y + a_4 \cdot x^2 + a_5 \cdot y^2$$
$$\Delta y = y' - y = b_0 + b_1 \cdot x + b_2 \cdot y + b_3 \cdot x \cdot y + b_4 \cdot x^2 + b_5 \cdot y^2 \tag{3}$$

where a_0 to a_5 and b_0 to b_5 are the adjustment parameters of an image, Δx and Δy express the discrepancies between the line measured and the sample coordinates for the new GCPs in the image space (x', y') and the RPCs projected coordinates for the same GCPs (x, y).

For the zero order transformation (RPC0), only a simple shift (a_0 and b_0) are computed. Because of it, only one GCP is necessary to calculate this indirect method. When an affine transformation in the image space is used (RPC1), six coefficients of Eq. (1) (a_0 to a_2 and b_0 to b_2) have to be computed. Therefore it is necessary to know at least three GCPs. Finally, besides RPC0 and RPC1, a third order 3D rational functions with vendor's RPCs data and refined by a second order polynomial adjustment (RPC2) is also tested in this work. In this case 12 coefficients (a_0 to a_5 and b_0 to b_5) have to be computed using, at least, six GCPs.

3.2. Geometric quality assessment tests

The geopositioning capabilities of GeoEye-1 and WV-2 PAN images have been studied, both after of the sensor orientation, and at the final orthorectification phase where the distorting affects of the terrain relief are removed using a DEM. OrthoEngine® was the software used in any case.

3.2.1. Direct geopositioning of GeoEye-1 and WorlView-2 products without GCPs

Direct georeferencing accuracies were performed within OrthoEngine® by only using the supplied RPCs. They were always calculated at 75 permanent ICPs and without the support of any GCP. Geometric accuracies were computed from the residuals attained at the 75 ICPs and presented as mean error and standard deviation.

3.2.2. Orientation accuracy assessment

The influence of some variables on the geometric accuracy at the orientation phase has been studied: (i) type of input VHR satellite PAN image (i.e., GeoEye-1 Geo, WV-2 Basic or WV-2 ORS2A), (ii) the sensor model (RPC0, RPC1, RPC2 and CCRS), (iii) the number of well-distributed GCPs used in the triangulation process ranging from 2 to 12, and (iv) off-nadir viewing angle ranging from 5° to 23.1°.

Several combinations of n GCPs (n = 2, 4, 7, 10, and 12) were generated from the 44 measured GCPs (Fig. 2). Five replicates were extracted over the study area for each number of GCPs (i.e., 25 different sets of GCPs), always looking for an even distribution both planimetric and vertical. The same sets of GCPs were used for each of the eight singles PAN images tested. So, and taking into account that some sensor models needed a minimum number of GCPs to be computed, 75 orientation projects were carried out for each single VHR satellite image (i.e., 25 projects for RPC0, 20 for RPC1, 15 for RPC2 and 15 projects for CCRS).

It is important to keep in mind that, for each image tested, the ground points were only marked once. On another note, all the residual populations at X and Y axes were tested for normality of their distribution. The Kolmogorov–Smirnov test was used as a goodness of fit to a standard normal distribution. Furthermore, no blunder errors were identified at the residual populations by applying the widely known 3-sigma rule (Daniel and Tennant, 2001).

In order to study the influence of the four aforementioned studied factors and their cross-interactions during the bundle adjustment phase regarding sensor orientation accuracy, an analysis of variance (ANOVA) test was carried out. The observed variable for the designed factorial model with five repetitions (Snedecor and Cochran, 1980) was the planimetric root mean square error ($RMSE_{2D}$) computed at the same 75 ICPs (Fig. 2). In this point, it is worth noting that, given such a high number of ICPs, the estimated error for $RMSE_{2D}$ calculation could reach values lower than 10% (Aguilar et al., 2008b). When the results of ANOVA test turned out to be significant, the separation of means was carried out using Duncan's multiple range test at a 95% confidence level.

3.2.3. Orthoimages accuracy

During the orthorectification phase, only six (three GeoEye-1 Geo and three WV-2 ORS2A images) out of the eight original satellite images were tested. For each of these six images, ten PAN orthoimages with GSD of 0.5 m were generated by combining RPC0 sensor model, the five sets of seven well-distributed GCPs and two different DEMs (the LiDAR-derived and the Andalusia DEM). Only 48 ICPs of the original 75 ICPs could be used for the geometric accuracy assessment at this phase, because of some ICPs on the orthoimages were located at corners of buildings and so, not placed on the bare ground. In the process of orthorectification, a sinusoidal resampling kernel ($\sin(x)/x$ with 16×16 windows) (Toutin, 2004) was applied to original image cells. Also an ANOVA test was carried out at this phase.

Table 2
Direct geopositioning accuracy at 75 ICPs presented as mean error and standard deviation (σ) for GeoEye-1 and WV-2 single images without GCPs support.

Image product	Off-nadir	Mean error (m)		σ (m)		
		X	Y	X	Y	2D
GeoEye-1 Geo	8.5°	1.87	3.00	0.23	0.21	0.31
	20.6°	2.65	0.57	0.21	0.26	0.33
	23.1°	1.80	3.47	0.28	0.25	0.38
WV-2 ORS2A	5°	1.85	0.15	0.24	0.24	0.34
	10°	−0.02	1.54	0.29	0.30	0.42
	22.4°	1.19	0.03	0.32	0.36	0.48
WV-2 Basic	10°	0.39	1.10	0.33	0.45	0.56
	22.4°	0.22	0.53	0.33	0.44	0.55

4. Results and discussion

4.1. Direct geopositioning of GeoEye-1 and WorlView-2 products without GCPs

Table 2 shows the direct geopositioning accuracy of each of the eight VHR satellite PAN images used in this work. Overall, geometric accuracies measured as standard deviations and computed in object point coordinates were higher for the GeoEye-1 Geo images, presenting a planimetric systematic error or bias always lesser than 4 m. On the other hand, biases lesser than 2 m were estimated from WV-2 ORS2A images and even better results were reached from WV-2 Basic images. The specified accuracy for both GeoEye-1 Geo and WV-2 Basic or ORS2A products is 5 m measured as Circular Error 90% (CE90) or 3 m $RMSE_{2D}$ (GeoEye, 2009; DigitalGlobe, 2011). In both cases, these nominal and systematical horizontal shifts would not be taking into account the terrain and off-nadir effects.

It is noted that, focusing on planimetry and mainly depending on the off-nadir angle, the uncertainty (measured as standard deviation) for the resulting coordinate errors in object space were ranging from 0.31 m to 0.38 m for GeoEye-1 Geo, whereas values from 0.34 m to 0.48 m were reached in the case of WV-2 ORS2A images. The highest planimetric standard deviations were attained from WV-2 Basic images. These values could be supposed as the best possible geopositioning accuracy results after applying bias corrections and they could be attained using only a few GCPs.

4.2. Accuracy assessment at sensor orientation phase

The first global ANOVA statistical test was developed using $RMSE_{2D}$ as observed variable on 600 different sensor orientation projects (e.g., 160 projects were carried out for 12, 10 and 7 GCPs by using four sensor models, eight satellite images and five repetitions, whereas 80 orientation projects for 4 GCPs corresponding to RPC0 and RPC1 sensor models were conducted, and finally, 40 projects for 2 GCPs were drawn up). The four main factors analyzed were significant ($p < 0.05$), being the sensor model used the most important source of variation in the ANOVA model presenting the highest F-test statistic with a value of 72.1, followed by the type of input VHR satellite PAN image (F-test = 30.9). The number of GCPs (F-test = 13.2) and the off-nadir viewing angle (F-test = 11.4) had a lesser repercussion regarding ANOVA results, but, anyway, both of them were also statistically significant. According to main factors cross-interactions, the crossed effects of sensor model with number of GCPs (F-test = 9.1) turned out to be significantly related ($p < 0.05$). This shows that the sensor models tested behavior differently with regard to the number of GCPs used, being RPC0 the sensor model more independent of that number. The type of input image with off-nadir angle (F-test = 5.7) also showed significantly crossed effects. Overall, WV-2 Basic images were slightly less affected by high off-nadir angles.

The $RMSE_{2D}$ values computed at sensor orientation phase are shown in Table 3. Note that each presented $RMSE_{2D}$ means the average value of five repetitions. For every type of input image, the best geopositioning accuracies were always attained by RPC0 and RPC1, being RPC2 and CCRS significantly ($p < 0.05$) worse. On the other hand, the results were significantly better when using GeoEye-1 Geo images than WV-2 ORS2A or WV-2 Basic ones. In this way, comparing only WV-2 images taken on August 18, 2011 (Table 4), the planimetric accuracies generated from ORS2A images were significantly better than the attained ones from Basic level, even for the rigorous model, what is notable taking into account the very limited metadata file contained in ORS2A images. Working with WorldView-1 stereo pairs and using RPC0 and RPC1 models, Chen and Chaapel (2008a) reported that OR2A level displayed more reliable results than Basic imagery. A comparison between WorldView-1 ORS2A and Basic single images at Spokane was carried out by Chen and Chaapel (2008b), reporting better planimetric accuracies at sensor orientation phase using ORS2A image ($RMSE_{2D}$ of 0.56 m and 0.64 m using RPC0 and RPC1 respectively) than those obtained from Basic level ($RMSE_{2D}$ around 1.04 m for RPC0 and RPC1). Because the DigitalGlobe's ORS2A product is map-projected, the effects of any high-frequency movement have already been removed from the scene, resulting in a much better fit for the RPC model. In addition, the ORS2A product can often be less expensive than the Basic product, since an ORS2A product can be made from any arbitrary area, as opposed to having to purchase the full scene. ORS2A products are also recommended for geometric correction because PAN and MS data are resampled to exactly the same geographic extents; hence, it is possible to perform pan-sharpening of the data before applying geometric correction if a pan-sharpened orthorectified image was desired. This fact, which is valid for GeoEye-1 Geo product too, gets that the sensor orientation results attained for PAN images could be directly extrapolated to the pan-sharpened images (Aguilar et al., 2012). The last is extremely desirable due to the availability of MS images from these VHR satellites has provided unique opportunities for several remote sensing applications. In this way, Aguilar et al. (2012) achieved geopositioning accuracies for the MS GeoEye-1 images measured as $RMSE_{2D}$ of around of 1.4 m (i.e., 0.7 pixels) using RPC0 with only four or seven GCPs.

With regard to the number of GCPs used, and returning to Table 3, it needs to be noted that, for every sensor model, $RMSE_{2D}$ values in the same column followed by different superscript letters are indicating significant differences at $p < 0.05$. So, and focusing on the case of RPC0 and GeoEye-1 Geo, the mean value for two GCPs (0.382 m) turned out to be statistically different as compared to 10 and 12 GCPs (the superscript letter is *b* for two GCPs whereas it is different, *a*, for 10 and 12 GCPs), but it did not when four or seven GCPs were used (the superscript letters are *ab* for four and seven GCPs). Thus, and in the case of RPC0 model, four GCPs would be the ideal statistic choice for GeoEye-1 images (i.e., the lowest number of GCPs without statistic difference with regard to the best accuracy mean value). In this way, seven would be the ideal number of GCPs working with both ORS2A and Basic WV-2 products. In the same way, and focusing on RPC1, it would be recommendable to use seven GCPs working with GeoEye-1 or WV-2 Basic imagery, and 10 GCPs for WV-2 ORS2A.

Table 3 also shows the statistical differences between RPC0 and RPC1 models for both GeoEye-1 Geo and WV-2 ORS2A images. As can be seen, all the four $RMSE_{2D}$ mean values compared for GeoEye-1 images were significant at 0.05 or 0.10 level, consistently showing better accuracies using RPC0. In this way, but now looking at WV-2 ORS2A product, although RPC0 also attained higher planimetric accuracies than RPC1 for every number of GCPs tested,

Table 3
Comparison of mean values of $RMSE_{2D}$ computed at 75 ICPs from GeoEye-1 Geo, WV-2 ORS2A and WV-2 Basic panchromatic images depending on the number of GCPs (No. GCPs). For each sensor model tested, values in the same column followed by different superscript letters indicate significant differences at a significance level $p < 0.05$. Mean values for RPC0 sensor model presented in bold indicate significant differences at $p < 0.05$ with regard to its corresponding mean value for RPC1 whereas the values presented in bold and italic indicate differences at $p < 0.10$ level.

Sensor model	No. GCPs	GeoEye-1 Geo $RMSE_{2D}$ (m)	WV-2 ORS2A $RMSE_{2D}$ (m)	WV-2 Basic $RMSE_{2D}$ (m)
RPC0	2	0.382^{a}	0.468^{a}	0.674^{a}
	4	$\mathbf{0.374^{ab}}$	$\mathbf{\textit{0.466}^{a}}$	0.659^{a}
	7	$\mathbf{\textit{0.368}^{ab}}$	$\mathbf{0.443^{b}}$	0.608^{b}
	10	$\mathbf{0.357^{b}}$	0.428^{b}	0.595^{b}
	12	$\mathbf{0.353^{b}}$	0.430^{b}	0.600^{b}
RPC1	4	0.452^{a}	0.501^{a}	0.675^{a}
	7	0.397^{b}	0.471^{a}	0.605^{b}
	10	0.394^{b}	0.438^{b}	0.592^{b}
	12	0.376^{b}	0.437^{b}	0.572^{b}
RPC2	7	0.554^{a}	0.618^{a}	0.825
	10	0.462^{ab}	0.527^{ab}	0.718
	12	0.405^{b}	0.479^{b}	0.636
CCRS	7	0.984^{a}	1.005^{a}	1.178
	10	0.545^{b}	0.709^{b}	0.814
	12	0.496^{b}	0.627^{b}	0.915

Table 4
Comparison of mean values of $RMSE_{2D}$ computed at 75 ICPs from WV-2 images taken on August 18, 2011 as ORS2A product as well as WV-2 Basic product (*N.S.S.* means no statistical significance).

Sensor model	Off-nadir	WV-2 product	$RMSE_{2D}$ (m)	Statistical significance
RPC0	10°	ORS2A	0.442	$p < 0.05$
		Basic	0.571	
	22.4°	ORS2A	0.534	$p < 0.05$
		Basic	0.600	
RPC1	10°	ORS2A	0.446	$p < 0.05$
		Basic	0.654	
	22.4°	ORS2A	0.572	$p < 0.05$
		Basic	0.650	
RPC2	10°	ORS2A	0.498	$p < 0.05$
		Basic	0.665	
	22.4°	ORS2A	0.695	$p < 0.05$
		Basic	0.788	
CCRS	10°	ORS2A	0.627	$p < 0.10$
		Basic	0.905	
	22.4°	ORS2A	0.951	*N.S.S.*
		Basic	1.033	

only in the case of 4 and 7 GCPs were observed significant differences. Several authors have pointed out that adding terms to the image-to-space transformation by using RPC1 or RPC2 instead of RPC0 could improve the accuracy of the results, but only when there are higher order distortions in the images (e.g., Fraser and Hanley, 2005; Shaker, 2008; Tong et al., 2010). In fact, RPC1 model worked slightly better than RPC0 only when it was applied to WV-2 Basic imagery. It is worth noting that WV-2 Basic images have not been totally corrected regarding small movements, wiggles or other shaking in the satellite platform during image acquisition, especially in the case of forward scanned images. Bearing in mind these results, it seems reasonable to recommend the RPC0 model for the sensor orientation phase if steadied VHR satellite PAN images such as GeoEye-1 Geo and WV-2 ORS2A are used. In fact, several researchers working on both satellite products have reported the RPC0 model as the most accurate and simple sensor model (Fraser and Ravanbakhsh, 2009; Meguro and Fraser, 2010; Chen and Chaapel, 2010). Moreover, its behavior results practically independent of the number and distribution of the GCPs used (Aguilar et al., 2012).

Table 5 shows detailed results at sensor orientation phase about planimetric accuracies attained from both GeoEye-1 Geo and WV-2 ORS2A panchromatic images depending on the off-nadir angle. Overall, for any sensor model and image product tested, $RMSE_{2D}$ mean values were higher with increasing off-nadir angle. It is well known that the image viewing angle has a great influence on the resulting orthorectified image (e.g., Toutin, 2004; Aguilar et al., 2006; Kapnias et al., 2008; Krystyna et al., 2011), but also on the accuracy attained at sensor orientation phase. The last would be related to an increase of both the collected GSD and the image pointing error with larger image look angles. In this way, Fig. 3 shows the relationship (second order polynomial) between the

Table 5
Comparison of mean values of $RMSE_{2D}$ from GeoEye-1 Geo and WV-2 ORS2A panchromatic images depending on the off-nadir angle. For each sensor model and image product tested, values in the same column followed by different superscript letters indicate significant differences at a significance level $p < 0.05$. Values for RPC0 sensor model presented in bold indicate significant differences at $p < 0.05$ level with regard to its corresponding value for RPC1.

Image product	Off-nadir	$RMSE_{2D}$ (m)			
		RPC0	RPC1	RPC2	CCRS
GeoEye-1 Geo	8.5°	$\mathbf{0.337^{a}}$	0.372^{a}	0.419^{a}	0.618^{a}
	20.6°	$\mathbf{0.357^{b}}$	0.372^{a}	0.439^{a}	0.653^{a}
	23.1°	$\mathbf{0.405^{c}}$	0.471^{b}	0.562^{b}	0.737^{a}
WV-2 ORS2A	5°	0.365^{a}	0.367^{a}	0.431^{a}	0.764^{ab}
	10°	0.442^{b}	0.446^{b}	0.498^{a}	0.627^{a}
	22.4°	$\mathbf{0.534^{c}}$	0.572^{c}	0.695^{b}	0.951^{b}

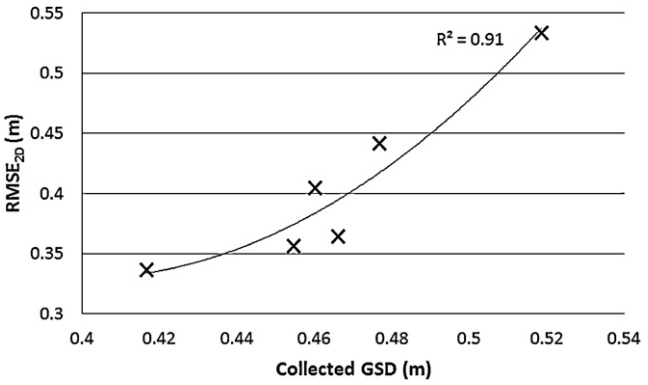

Fig. 3. Relationship between the collected GSD and the $RMSE_{2D}$ attained at the sensor orientation phase by using RPC0 for GeoEye-1 Geo and WV-2 ORS2A images.

real or collected GSD (average of Collected Col GSD and Collected Row GSD in Table 1) and the accuracy attained at the sensor orientation phase by using RPC0 for GeoEye-1 Geo and WV-2 ORS2A images. Again, the best sensor model was RPC0, especially for all the three GeoEye-1 images, being in these cases statistically significant ($p < 0.05$) compared to RPC1.

It has to be emphasized that the best planimetric accuracies mean values attained by using RPC0 for every single image presented in Table 5 were always very close to the best possible geopositioning accuracies shown as planimetric standard deviations in Table 2. Based on nearly a decade of experience with VHR satellites, planimetric geopositioning accuracy to around 0.5–0.7 pixels would be readily achievable by using refined RPCs with a few high accuracy GCPs (Fraser and Ravanbakhsh, 2009). In this study, and for GeoEye-1 Geo images with a product pixel size of 0.5 m, mean $RMSE_{2D}$ values of 0.67, 0.72 and 0.81 pixels were attained by using RPC0 on growing off-nadir angles of 8.5°, 20.6° and 23.1° respectively. On the other hand, and for every WV-2 ORS2A image (product pixel size of 0.5 m), slightly worse mean $RMSE_{2D}$ values of 0.73, 0.88 and 1.01 pixels were computed from off-nadir angles of 5°, 10° and 22.4° respectively.

At sensor orientation phase, Teo (2011) attained planimetric accuracies around 0.84 pixels from a basic WV-2 single image with an off-nadir of 8.6°. Meguro and Fraser (2010) reported planimetric accuracies close to 0.7 pixels by using a stereo pair of pan-sharpened GeoEye-1 images and RPC0 model, whereas Wang and Zhao (2011), using 5 GCPs and RPC0, attained 0.38 m (0.76 pixels) as planimetric accuracy. On the other hand, also working with a stereo pair of GeoEye-1 and RPC0, Fraser and Ravanbakhsh (2009) achieved horizontal accuracies of 0.2 pixels, but in this case, supported by extremely accurate measured ground points, both in object and image space.

With regard to the physical sensor model tested and from comparing it against models based on RPCs, very poor results have been found for both GeoEye-1 and WV-2 products. In addition, poor sensor orientation accuracies were also reported working with GeoEye-1 (e.g., Crespi et al., 2010) and WV-2 (e.g., Deltsidis and Ioannidis, 2011; Krystyna et al., 2011) imagery. However, good accuracies using a rigorous model included in the SISAR software were achieved by Capaldo et al. (2012) working with stereo pairs from WV-1 and GeoEye-1 achieved.

4.3. Accuracy assessment of orthoimages

Table 6 shows the mean values of the two-dimensional accuracy computed from orthorectified GeoEye-1 Geo and WV-2 ORS2A images using two different DEMs. When a very accurate LiDAR-derived DEM (vertical accuracy close to 0.09 m) was used to carry out the orthorectification process, significantly better planimetric accuracies were achieved as compared to the orthoimages produced from the Andalusia DEM (vertical accuracy close to 1.34 m). Also, and working on GeoEye-1 Geo images, the corresponding orthoimages presented a slightly better geometric accuracy than those generated from WV-2 ORS2A, especially when using very high off-nadir angles. In this way, the off-nadir viewing angle had a significant ($p < 0.05$) effect on orthoimages accuracy, attaining higher $RMSE_{2D}$ values with increasing off-nadir angles.

The orthoimages attained by using the LiDAR-derived DEM yielded planimetric accuracies ranging from 0.40 m to 0.63 m, whereas the $RMSE_{2D}$ raised up to values of between 0.50 m and 0.95 m when the Andalusia DEM was employed (Table 6). In this way, the choice of a very accurate DEM has a lot of importance on the final orthoimage geopositioning accuracy, especially when images with high off-nadir angles are used. As can be seen in Table 6, a $RMSE_{2D}$ mean value of 0.95 m was attained from the orthorectified WV-2 image corresponding to the highest off-nadir and medium resolution DEM, whereas the planimetic accuracy was drastically increased when the LiDAR-derived DEM was applied. In other words, the high off-nadir angle should only be used with very accurate DEMs when high accuracies in the final orthoimages are needed. When only medium resolution DEMs are able for the orthorectification process, the satellite images should be order with the highest possible elevation angle (i.e., the smallest off-nadir angle). In this regard, customers can upgrade the target elevation angle to be between 72° and 90° for an additional fee in the GeoEye products order form (GeoEye, 2009) to increase the positional accuracy of the final orthorectified imagery. It is noteworthy that, using a 0.6 m vertical accuracy DEM, $RMSE_{2D}$ values of 0.74 m, 1.11 m and 1.07 m were attained by Krystyna et al. (2011) working on WV-2 ORS2A single images presenting off-nadir angles of 26.7°, 31.6° and 36° respectively, being RPC0 the best of the tested sensor models.

Table 6 also shows the standard deviations of the $RMSE_{2D}$ mean values (five replications). As can be noted, the small standard deviation values indicate a high reliability for the orthoimages geometric accuracy assessment carried out along this work. Overall, the

Table 6
Mean or average values and standard deviations computed for $RMSE_{2D}$ accuracies (five repetitions) on the orthorectified GeoEye-1 Geo and WV-2 ORS2A imagery (48 ICPs) by using RPC0 model and seven GCPs. For each DEM and image product tested, mean values in the same column followed by different superscript letters indicate significant differences at a significance level $p < 0.05$.

Image product	Off-nadir	Orthoimage LiDAR DEM ICPs $RMSE_{2D}$ (m)		Orthoimage Andalusia DEM ICPs $RMSE_{2D}$ (m)	
		Mean	σ	Mean	σ
GeoEye-1 Geo	8.5°	0.404^{a}	0.027	0.546^{a}	0.038
	20.6°	0.464^{b}	0.021	0.622^{b}	0.016
	23.1°	0.501^{c}	0.025	0.689^{c}	0.048
WV-2 ORS2A	5°	0.425^{a}	0.010	0.501^{a}	0.022
	10°	0.462^{a}	0.019	0.584^{b}	0.039
	22.4°	0.632^{b}	0.055	0.951^{c}	0.093

highest standard deviation values were associated to high off-nadir angles and low accuracy DEM.

In any case, and within our small and very smooth relief study area, the orthorectification process of VHR satellite images with off-nadir angles lesser than 15° only would need the Andalusia DEM for attaining planimetric accuracies ranging from 0.50 to 0.58 m. When sub-pixel accuracy is required, a more accurate DEM should be used, avoiding, whenever possible, high off-nadir angles.

Although one-dimensional accuracies ($RMSE_x$ and $RMSE_y$) are not presented here, it is worth mentioning that slight along-track biases were detected in some of the images tested, mainly in the orthoimages, but also at orientation phase. In fact, the most substantial biases found in orthoimages were presented when the Andalusia DEM and off-nadir angles of 23.1° and 22.4° for both GeoEye-1 Geo and WV-2 ORS2A products were used. These along-track biases have been already reported for QuickBird and Ikonos images (Noguchi et al., 2004; Fraser and Hanley, 2005; Aguilar et al., 2007).

5. Conclusions

The impressive direct geopositioning accuracy attained without GCPs for the newest VHR satellites tested in this work proves the notably improvement carried out on the sensor camera model given by the corresponding RPCs. However, when the best geometric accuracy is required for the final orthoimage computed from GeoEye-1 or WV-2 satellites, the RPC bundle adjustment refined with a few GCPs and a high accurate DEM must be used.

In this way, and working under operational conditions, RPC0 sensor model attained the best significant ($p < 0.05$) geopositioning accuracy at orientation phase using both GeoEye-1 and WV-2 single images. A number of GCPs ranging from 4 to 7 would be recommended for attaining the best results by using RPC0 model. In this sense, sub-pixel geopositioning accuracies might be achieved both for GeoEye-1 and WV-2 images, although, from the test cases examined, GeoEye-1 Geo images yielded slightly higher planimetric accuracy than WV-2 ORS2A or WV-2 Basic ones. Regarding the WV-2 products tested, the planimetric accuracies at sensor orientation phase computed from WV-2 ORS2A images were significantly better than those attained from Basic level.

With regard to the corresponding orthoimages, similar results were found from GeoEye-1 Geo and WV-2 ORS2A single images presenting an off-nadir angle lesser than 20°. It was proved that higher $RMSE_{2D}$ values were related to increasing off-nadir viewing angle. By using RPC0 model, seven well distributed GCPs and avoiding the two single images with the highest off-nadir, orthoimages with sub-pixel planimetric accuracy were attained by means of a very accurate LiDAR-derived DEM for both GeoEye-1 Geo and WV-2 ORS2A single images. However, and in the same conditions but using a much less accurate photogrammetrically derived DEM, planimetric accuracies ranging from 0.50 m to 0.62 m were obtained.

Keeping in mind the extremely accurate geopositioning reported by Fraser and Ravanbakhsh (2009) working on a stereo pair of GeoEye-1, probably the results achieved in this study might be still improved by mainly cutting down the pointing error of the GCPs marked in space image.

Although this work is focused on VHR satellite single PAN images, the availability of MS images from these satellites should not be forgotten. In that sense, when WV-2 ORS2A or GeoEye-1 Geo products are used, the results presented here would be directly extrapolated to the pan-sharpened images attained merging and combining the PAN and MS bands. Further works would be advisable to test the geopositioning accuracy capabilities of MS images from WV-2 and GeoEye-1.

Acknowledgements

This work was supported by the Spanish Ministry for Science and Innovation (Spanish Government) and the European Union (FEDER founds) under Grant Reference CTM2010-16573. The authors also appreciate the support from Andalusia Regional Government, Spain, through the Excellence Research Project RNM-3575.

References

Aguilar, F.J., Aguilar, M.A., Carvajal, F., Agüera, F., 2006. An integrated model to estimate the accuracy of digital orthoimages from high resolution satellite imagery. Revue Française de Photogrammétrie et de Télédétection 184, 11–16.

Aguilar, M.A., Aguilar, F.J., Agüera, F., Sánchez, J.A., 2007. Geometric accuracy assessment of QuickBird basic imagery using different operational approaches. Photogrammetric Engineering & Remote Sensing 73 (12), 1321–1332.

Aguilar, M.A., Agüera, F., Aguilar, F.J., Carvajal, F., 2008a. Geometric accuracy assessment of the orthorectification process from very high resolution satellite imagery for Common Agricultural Policy purposes. International Journal of Remote Sensing 29 (24), 7181–7197.

Aguilar, M.A., Aguilar, F.J., Agüera, F., 2008b. Assessing geometric reliability of corrected images from very high resolution satellites. Photogrammetric Engineering & Remote Sensing 74 (12), 1551–1560.

Aguilar, M.A., Aguilar, F.J., Saldaña, M.M., Fernández, I., 2012. Geopositioning accuracy assessment of GeoEye-1 panchromatic and multispectral imagery. Photogrammetric Engineering & Remote Sensing 78 (3), 7181–7197.

Andalusia Government, 2005. Modelo Digital del Terreno de Andalucía. Relieve y Orografia. Junta de Andalucía, Sevilla, Spain (on DVD).

Capaldo, P., Crespi, M., Fratarcangeli, F., Nascetti, A., Pieralice, F., 2012. DSM generation from high resolution imagery: applications with WorldView-1 and Geoeye-1. Italian Journal of Remote Sensing 44 (1), 41–53.

Chen, P., Chaapel, C., 2008a. Automatic DEM generation using WorldView-1 stereo data with or without ground control. GeoInformatics 7, 34–39.

Chen, P., Chaapel, C., 2008b. Increased image collection opportunities DigitalGlobe's WorldView-1 satellite. GeoInformatics 3, 16–21.

Chen, P., Chaapel, C., 2010. Pan-sharpening and geometric correction WorldView-2 satellite. GeoInformatics 4, 30–33.

Crespi, M., Capaldo, P., Fratarcangeli, F., Nascetti, A., Pieralice, F., 2010. DSM generation from very high optical and radar sensors: problems and potentialities along the road from the 3D geometric modeling to the surface model. In: 30th IEEE International Geoscience and Remote Sensing Symposium, IGARSS, 2010, 25–30 July, Honolulu, U.S.A, pp. 3596–3599.

Daniel, C., Tennant, K., 2001. DEM quality assessment. In: Maune, D.F. (Ed.), Digital Elevation Model Technologies and Applications: The DEM Users Manual. American Society for Photogrammetry & Remote Sensing, Bethesda, Maryland, pp. 395–440.

Deltsidis, P., Ioannidis, C., 2011. Orthorectification of WorldView-2 stereo pair using a new rigorous orientation model. In: Heipke, C., Jacobsen, K., Rottensteiner, F., Müller, S., Sörgel, U. (Eds.), ISPRS Hannover Workshop 2011: High-Resolution Earth Imaging for Geospatial Information. June 14–17, 2011, Hannover, Germany.

Dennison, P.E., Brunelle, A.R., Carter, V.A., 2010. Assessing canopy mortality during a mountain pine beetle outbreak using GeoEye-1 high spatial resolution satellite data. Remote Sensing of Environment 114, 2431–2435.

DigitalGlobe, Inc., 2010. DigitalGlobe Core Imagery Products Guide. http://www.digitalglobe.com/downloads/DigitalGlobe_Core_Imagery_Products_Guide.pdf (accessed 19.04.12).

DigitalGlobe, Inc., 2011. DigitalGlobe Basic Imagery. http://www.digitalglobe.com/downloads/BasicImagery-DS-BASIC-Web.pdf (accessed 03.02.12).

Dolloff, J., Settergren, R., 2010. An assessment of WorldView-1 positional accuracy based on fifty contiguous stereo pairs of imagery. Photogrammetric Engineering & Remote Sensing 76 (8), 935–943.

Fraser, C.S., Hanley, H.B., 2005. Bias-compensated RPCs for sensor orientation of high-resolution satellite imagery. Photogrammetric Engineering & Remote Sensing 71 (8), 909–915.

Fraser, C.S., Ravanbakhsh, M., 2009. Georeferencing accuracy of GeoEye-1 imagery. Photogrammetric Engineering & Remote Sensing 75 (6), 634–638.

GeoEye, Inc., 2009. GeoEye Product Guide. http://www.geoeye.com/CorpSite/assets/docs/brochures/GeoEye_Product_Guide.pdf (accessed 03.02.12).

Grodecki, J., Dial, G., 2003. Block adjustment of high-resolution satellite images described by rational polynomials. Photogrammetric Engineering & Remote Sensing 69 (1), 59–68.

Kapnias, D., Milenov, P., Kay, S., 2008. Guidelines for Best Practice and Quality Checking of Ortho Imagery, Issue 3.0. European Commission, JRC Scientific and Technical Reports EUR 23638 EN-2008.

Krystyna, J., Da Costa, N., Walczyńska, A., 2011. Geometric Quality Testing of the WorldView-2 Image Data Acquired over the JRC Maussane Test Site using ERDAS LPS, PCI Geomatics and Keystone Digital Photogrammetry Software Packages – Initial Findings with ANNEX. European Commission, JRC Scientific and Technical Reports EUR 24525 EN-2011.

Meguro, Y., Fraser, C.S., 2010. Georeferencing accuracy of GeoEye-1 stereo imagery: experiences in a Japanese test field. International Archives of the

Photogrammetry, Remote Sensing and Spatial Information Sciences 38 (8), 1069–1072.
Noguchi, M., Fraser, C.S., Nakamura, T., Shimono, T., Oki, S., 2004. Accuracy assessment of QuickBird stereo imagery. Photogrammetric Record 19 (106), 128–137.
Ozdemira, I., Karnieli, A., 2011. Predicting forest structural parameters using the image texture derived from WorldView-2 multispectral imagery in a Dryland forest, Israel. International Journal of Applied Earth Observation and Geoinformation 13, 701–710.
Shaker, A., 2008. Satellite sensor modeling and 3D geo-positioning using empirical models. International Journal of Applied Earth Observation and Geoinformation 10, 282–295.
Snedecor, G.W., Cochran, W.G., 1980. Statistical Methods, seventh ed. Iowa State University Press, Ames, IA, 507 pp.
Tao, C.V., Hu, Y., 2001. A comprehensive study of the rational function model for photogrammetric processing. Photogrammetric Engineering & Remote Sensing 67 (12), 1347–1357.
Teo, T., 2011. Bias compensation in a rigorous sensor model and rational function model for high-resolution satellite images. Photogrammetric Engineering & Remote Sensing 77 (12), 1211–1220.
Tong, X., Liu, S., Weng, Q., 2010. Bias-corrected rational polynomial coefficients for high accuracy geo-positioning of QuickBird stereo imagery. ISPRS Journal of Photogrammetry and Remote Sensing 65, 218–226.
Toutin, T., 2003. Error tracking in Ikonos geometric processing using a 3D parametric model. Photogrammetric Engineering & Remote Sensing 69 (1), 43–51.
Toutin, T., 2004. Review article: geometric processing of remote sensing images: models, algorithms and methods. International Journal of Remote Sensing 25 (10), 1893–1924.
Valadan Zoej, M.J., Mokhtarzade, M., Mansourian, A., Ebadi, H., Sadeghian, S., 2007. Rational function optimization using genetic algorithms. International Journal of Applied Earth Observation and Geoinformation 9, 403–413.
Wang, W., Zhao, L., 2011. Geolocation Accuracy Evaluation of GeoEye-1 Stereo Image Pair. In: International Symposium on Image and Data Fusion, ISIDF, Yunnan, China (Conference papers from IEEEXplore).
Wolniewicz, W., 2004. Assessment of geometric accuracy of VHR satellite images. In: Proceeding of the XXth International Archives of the Photogrammetry, Remote Sensing and Spatial Information Sciences, 12–23 July, Istanbul, Turkey, vol. 35 (Part B1) (unpaginated CD-ROM).